JACC: CARDIOVASCULAR IMAGING
VOL. 5, NO. 11, 2012

ISSN 1936-878X/$36.00
PUBLISHED BY ELSEVIER INC.
http://dx.doi.org/10.1016/j.jcmg.2012.09.004

Combined CT Coronary Angiography and Stress Myocardial Perfusion Imaging for Hemodynamically Significant Stenoses in Patients With Suspected Coronary Artery Disease

A Comparison With Fractional Flow Reserve

Brian S. Ko, MBBS,* James D. Cameron, MD,* Michael Leung, PhD,*
Ian T. Meredith, PhD,* Darryl P. Leong, PhD,† Paul R. Antonis, MBBS,*
Marcus Crossett, BSc,*‡ John Troupis, MBBS,*‡ Richard Harper, MBBS,*
Yuvaraj Malaiapan, MBBS,* Sujith K. Seneviratne, MBBS*

Melbourne, Victoria, and Adelaide, South Australia, Australia

OBJECTIVES We sought to determine the accuracy of combined coronary computed tomography angiography (CTA) and computed tomography stress myocardial perfusion imaging (CTP) in the detection of hemodynamically significant stenoses using fractional flow reserve (FFR) as a reference standard in patients with suspected coronary artery disease.

BACKGROUND CTP can be qualitatively assessed by visual interpretation or quantified by the transmural perfusion ratio determined as the ratio of subendocardial to subepicardial contrast attenuation. The incremental value of each technique in addition to coronary CTA to detect hemodynamically significant stenoses is not known.

METHODS Forty symptomatic patients underwent FFR and 320-detector computed tomography assessment including coronary CTA and CTP. Myocardial perfusion was assessed using the transmural perfusion ratio and visual perfusion assessment. Computed tomography images were assessed by consensus of 2 observers. Transmural perfusion ratio ◻ 0.99 was used as the threshold for abnormal perfusion. FFR ≤0.8 indicated hemodynamically significant stenoses.

RESULTS Coronary CTA detected FFR-significant stenoses with 95% sensitivity and 78% specificity. The additional use of visual perfusion assessment and the transmural perfusion ratio both increased the specificity to 95%, with sensitivity of 87% and 71%, respectively. The area under the receiver-operating characteristic curve for coronary CTA ◻ visual perfusion assessment was significantly higher than both coronary CTA (0.93 vs. 0.85, p ◻ 0.0003) and coronary CTA ◻ the transmural perfusion ratio (0.93 vs. 0.79, p ◻ 0.0003). Per-vessel and per-patient accuracy for coronary CTA, coronary CTA ◻ the transmural perfusion ratio, and coronary CTA ◻ visual perfusion assessment was 83% and 83%, 87% and 92%, and 92% and 95%, respectively.

CONCLUSIONS In suspected coronary artery disease, combined coronary CTA ◻ CTP identifies patients with hemodynamically significant stenoses with ◻ 90% accuracy compared with FFR. When interpreted with coronary CTA, visual perfusion assessment provided superior incremental value in the detection of FFR-significant stenoses compared with the quantitative transmural perfusion ratio assessment. (J Am Coll Cardiol Img 2012;5:1097–111) © 2012 by the American College of Cardiology Foundation

Coronary computed tomography angiography (CTA) is a robust noninvasive method for the accurate diagnosis of coronary artery disease (CAD) with both sensitivity and negative predictive value (NPV) in excess of 94% for excluding significant stenoses (1). The specificity of coronary CTA in detecting hemodynamically significant coronary stenoses, however, is considerably lower and has been reported to range from 48% to 78% (2–4).

See page 1112

Computed tomography stress perfusion imaging (CTP) is an emerging method that can be used to detect myocardial ischemia. In patients with known CAD, we and others have shown that the added use of CTP may improve the accuracy of coronary CTA in the detection of hemodynamically significant stenoses (3,4). In symptomatic patients with suspected CAD, however, the role of CTP and its incremental value in addition to coronary CTA remain uncertain. This question is particularly relevant to the large population of patients with low to intermediate risk of CAD in whom coronary CTA is recommended as an appropriate and pivotal investigation (5).

A potential advantage in combined coronary CTA and CTP is the opportunity that it provides for the computed tomography (CT) interpreter to assess coronary anatomy and myocardial perfusion in the same setting. Accordingly, recent guidelines for CT perfusion interpretation recommend the use of up-front evaluation of stenoses on coronary CTA followed by perfusion assessment by the same reader (6) in preference to separate blinded interpretations of coronary CTA and CTP, which had occurred in early feasibility studies (7,8). Perfusion on CT can be qualitatively assessed by visual interpretation or quantified as the transmural perfusion ratio determined as the ratio of subendocardial to subepicardial contrast attenuation (7). To date, a comparison of the incremental value of qualitative versus quantitative perfusion assessment when used and interpreted in addition to coronary CTA has not been reported.

Our primary aim was to determine the incremental value of CTP assessed by qualitative and quantitative techniques when used and interpreted in combination with coronary CTA to detect hemodynamically significant stenoses in symptomatic patients with suspected CAD. Fractional flow reserve (FFR), a well-established and highly accurate invasive method to assess the functional significance of coronary stenoses, was used as the reference standard.

ABBREVIATIONS AND ACRONYMS

AUC = area under the curve
CAD = coronary artery disease
CI = confidence interval
CTA = computed tomography angiography
CTP = computed tomography stress myocardial perfusion imaging
FFR = fractional flow reserve
ICA = invasive coronary angiography
IDI = integrated discrimination improvement
LAD = left anterior descending artery
LCx = left circumflex artery
NPV = negative predictive value
PPV = positive predictive value
RCA = right coronary artery
ROC = receiver-operating characteristic

METHODS

From December 2010 to June 2011, we prospectively recruited symptomatic patients with no previously identified CAD who were referred for elective invasive coronary angiography (ICA). On the basis of the patient's age, sex, and symptoms (9), all were at intermediate or high risk of CAD as determined by the American Heart Association guidelines for chronic stable angina (10). Exclusion criteria included younger than 40 years of age, atrial fibrillation, high-grade atrioventricular block, renal insufficiency (estimated glomerular filtration rate ▫ 60 ml/min/1.73 m^2), bronchospastic lung disease requiring long-term steroid therapy, morbid obesity (body mass index ≥40 kg/m^2), and contraindications to iodinated contrast. Patients were scheduled for cardiac CT, including coronary CTA and CTP, within 14 days before ICA. At the time of ICA, the FFR was measured in all major patent epicardial coronary arteries. The study was approved by the institutional human research ethics committee, and all participants gave written informed consent.

CT imaging protocol. Patients underwent cardiac CT assessment using a 320-row detector CT scanner (Aquilion ONE, Toshiba Medical Systems, Tochigi, Japan). The CT protocol consisted of rest coronary CTA followed by CTP. Antianginal medications apart from beta-blockers were stopped 48 h before scanning. Additional beta-blockers were administered when indicated to achieve a pre-scan heart rate of ▫ 60 beats/min. For coronary CTA, a

From the *Monash Cardiovascular Research Centre, MonashHeart, Department of Medicine, Monash Medical Centre, Southern Health and Monash University, Melbourne, Victoria, Australia; †Discipline of Medicine, University of Adelaide, Adelaide, South Australia, Australia; and the ‡Department of Diagnostic Imaging, Monash Medical Centre, Southern Health and Monash University, Melbourne, Victoria, Australia. Dr. Ko is supported by a scholarship funded by the Royal Australasian College of Physicians. Dr. Leong is supported by a training fellowship cofunded by the National Health and Medical Research Council of Australia and the National Heart Foundation of Australia. Dr. Seneviratne has been a speaker at meetings sponsored by Toshiba. All other authors have reported that they have no relationships relevant to the contents of this paper to disclose.

Manuscript received July 18, 2012; revised manuscript received September 20, 2012, accepted September 24, 2012.

bolus of 55 ml of 100% iohexol 56.6 g/75 ml (Omnipaque 350, GE Healthcare USA) was injected into an antecubital vein at a flow rate of 5 ml/s, followed by 20 ml of a 30:70 mixture of contrast and saline solution, followed by 30 ml of saline solution. Scanning was triggered in the arterial phase using automated contrast bolus tracking with a region of interest placed in the descending aorta and automatically triggered at 300 Hounsfield units. Scan parameters for rest coronary CTA were as follows: detector collimation, 320 □ 0.5 mm; tube current, 300 to 500 mA (depending on body mass index); tube voltage, 120 kV; gantry rotation time, 350 ms; and temporal resolution, 175 ms. Prospective electrocardiographic gating was used covering phases 70% to 80% of the R-R interval. For images acquired at heart rates of ≤65 beats/min, scanning was completed with a single R-R interval using a 180° segment. In patients with a heart rate □ 65 beats/min, data segments from 2 consecutive beats were used for multisegment reconstruction with improved temporal resolution of 87 ms. The stress perfusion scan was performed 20 min after coronary CTA with intravenous adenosine infusion (140 μg/kg/min for 3 min), using prospective electrocardiographic gating covering phases 70% to 95% of the R-R interval, tube settings, and contrast dose as for the rest scan. The effective radiation dose was calculated by multiplying the dose-length product by a constant (k □ 0.014 mSv/mGy/cm) (11).

Image reconstruction and analysis. All CT images were analyzed on a dedicated workstation (Vitrea Fx 6.2, Vital Images, Minnetonka, Minnesota) by 2 experienced CT angiographers (S.K.S., M.L.) blinded to the results of ICA and FFR. The coronary CTA images were interpreted first, followed by perfusion assessment (6) (Fig. 1). All vessels with a diameter of ≥1.5 mm were analyzed using a 19-coronary segment model, as previously described (12). Each coronary segment was visually assessed for the degree of luminal stenosis, and a vessel was considered significantly stenosed if there was ≥1 segment that was nonassessable or with ≥50% luminal stenosis.

Perfusion assessment was performed using both the stress and rest images. Datasets were reconstructed at 3% R-R intervals using a reconstruction kernel (FC03), which incorporates beam hardening correction (6). The phase with the least cardiac motion was selected, and images were interpreted using a narrow window width and level setting (W300/L150) and an averaged multiplanar reconstruction slice thickness of 3 to 5 mm, according to the American Heart Association 17-myocardial segment model (13) with disagreement resolved by a third reader (B.S.K.). Segments with significant overlying artifacts were deemed uninterpretable and excluded from analysis.

For visual perfusion assessment, each segment was scored for the absence or presence of a perfusion defect. Defects were classified as transmural (≥50% myocardial wall thickness) or nontransmural (□ 50% wall thickness) and assessed for reversibility, image quality (defined as 1 □ poor, 2 □ moderate, 3 □ good) and reader confidence in defect identification (defined as 1 □ very certain, 2 □ rather certain, 3 □ uncertain , 4 □ very uncertain).

For quantitative assessment, the transmural perfusion ratio was calculated by readers blinded to the findings of visual perfusion assessment. The transmural perfusion ratio was scored for each segment, apart from the apex, using custom analysis software (Vitrea Fx 6.2, Vital Images). Images were displayed in the cardiac short axis, and an automated border detection algorithm was applied to define the subendocardial and subepicardial borders after manual adjustments to the left ventricular axis and myocardial contouring. The myocardium is divided into 3 myocardial layers (i.e., the subendocardium, midmyocardium, and subepicardial layers), and the attenuation density in each layer was calculated. The transmural perfusion ratio is calculated as the ratio of the segment-specific subendocardial attenuation density to the mean attenuation density of the entire subepicardial layer of any given short-axis slice. The segment with the lowest transmural perfusion ratio value was chosen to represent perfusion for each major vessel.

Each myocardial segment was specifically matched to its subtending major epicardial artery, as determined by the course of the artery and its branches on coronary CTA. For the combined coronary CTA □ CTP analysis, vessels were considered hemodynamically significant when coronary CTA demonstrated ≥50% stenosis, which was associated with a transmural perfusion ratio □ 0.99 (7) or a reversible perfusion defect in the vessels' subtended territory.

Invasive angiography and FFR. Invasive coronary angiography was performed as per standard practice either via the femoral or radial approach. The pressure wire (Pressure Wire Certus 6, St. Jude Medical, Uppsala, Sweden) was calibrated and electronically equalized with the aortic pressure before being placed in the distal third of the coronary

JACC: CARDIOVASCULAR IMAGING, VOL. 5, NO. 11, 2012
NOVEMBER 2012:1097–111

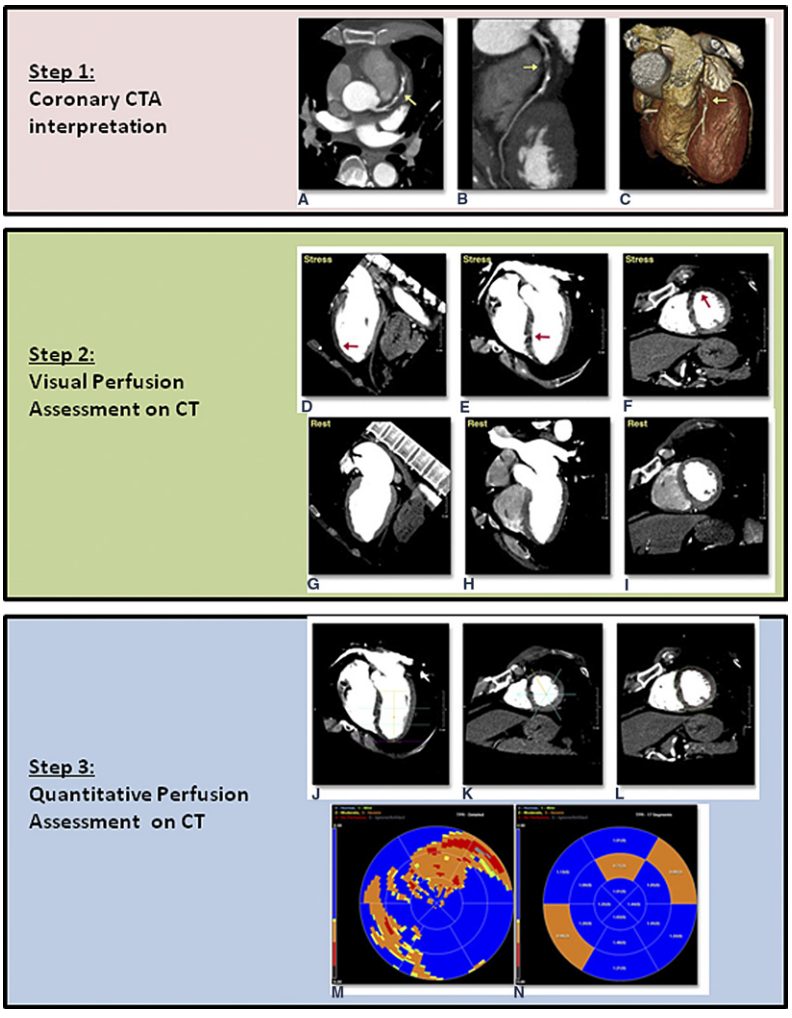

Figure 1. Combined Coronary CTA and CT Myocardial Perfusion Assessment Method

Step 1: Coronary computed tomography angiography (CTA) interpretation **(A, B)**. Each myocardial segment is then matched to its subtending artery using the volume-rendered image **(C)**. Step 2: Visual perfusion assessment on computed tomography (CT) is performed immediately after coronary CTA interpretation. The myocardium is examined for artifacts. The stress **(D to F)** and rest **(G to I)** images are then aligned and examined for reversible perfusion defects. Step 3: Quantitative perfusion assessment on CT. The myocardium is subdivided into the basal, mid, and apical segments **(J)**. After adjusting for left ventricular axis and myocardial contouring **(J to L)**, the transmural perfusion ratio is calculated using dedicated computer software (Vitrea Fx 6.2, Vital Images) and displayed in a color-coded polar plot in pixel format or averaged per myocardial segment **(M, N)**. A transmural perfusion ratio ▫ 0.99 is taken as abnormal perfusion. In this case, there was a critical proximal stenosis in the left anterior descending artery **(arrows in A to C)**. This was associated with reversible perfusion defects in the entire anterior septum and anterior walls **(arrows in D to F)**. The transmural perfusion ratio polar plot confirmed abnormal perfusion in the anterior and septal walls, with the lowest transmural perfusion ratio value of 0.71 **(M, N)**.

artery being interrogated. Intracoronary glyceryl trinitrate (100 μg) was injected to minimize vasospasm. Intravenous adenosine was administered (140 μg/kg/min) through an intravenous line in the antecubital fossa. At steady-state hyperemia, the FFR was recorded on a RadiAnalyzer Xpress (Radi Medical Systems, Uppsala, Sweden), calculated by dividing the mean coronary pressure measured with the pressure sensor placed distal to the stenosis by the mean aortic pressure measured through the guide catheter. This procedure was repeated for all major vessels. Arteries were recorded as having an FFR ≤0.8 if they had ▫ 90% stenosis on visual assessment, and an FFR ▫ 0.8 if they were smooth or had only minor irregularities (14). An FFR value of ≤0.8 was taken to define hemodynamically significant stenoses (15).

Quantitative coronary angiography. Quantitative coronary angiography was performed on all coronary arteries ≥1.5 mm in diameter using a 19-

Table 1. Patient Characteristics (N = 40)

Age, yrs	62.1 ▫ 9.9
Male	67.5 (27)
Body mass index, kg/m^2	28.2 ▫ 4.9
Creatinine, mmol/l	82.1 ▫ 19.6
Symptom*	
Typical angina	45.0 (18)
Atypical angina	22.5 (9)
Noncardiac chest pain	32.5 (13)
Pre-test risk of CAD†	
Intermediate risk of CAD	55.0 (22)
High risk of CAD	45.0 (18)
Cardiovascular risk factors	
Hypertension‡	75.0 (30)
Hyperlipidemia§	80.0 (32)
Current smoker	15.0 (6)
Diabetes	12.5 (5)
Family history of IHD	27.5 (11)
Obesity‖	30.0 (12)
Medication	
Aspirin	75.0 (30)
Clopidogrel	7.5 (3)
Beta-blocker	60.0 (24)
ACE inhibitor	17.5 (7)
ARB	32.5 (13)
Statin	67.5 (27)
Nitrates	7.5 (3)
Calcium channel blocker	30.0 (12)

Values are mean ▫ SD or % (n). *Determined in accordance with 2002 American Heart Association guidelines for chronic stable angina (10). †Pretest risk of coronary artery disease and symptoms. ‡Blood pressure ▫ 140/90 mm Hg or treatment for hypertension. §Total cholesterol ▫ 180 mg/dl or treatment for hypercholesterolemia. ‖Body mass index ▫ 30 kg/m^2.
ACE ▫ angiotensin-converting enzyme; ARB ▫ angiotensin receptor blocker; IHD ▫ ischemic heart disease.

segment coronary model (12). This was performed using a semiautomated edge detection system (Xcelera Cath R3.2, Philips, Best, the Netherlands) by 2 experienced cardiologists (B.S.K., P.R.A.) who were blinded to FFR and CT findings with disagreement resolved by consensus. Each coronary segment was assessed for the degree of luminal stenosis, and a vessel was considered significant if there was ≥1 segment that was nonassessable or with ≥50% luminal stenosis.

Statistical analysis. Continuous variables are presented as mean ▫ SD if normally distributed. Categorical variables are displayed as frequency (percentage). Sensitivity, specificity, positive predictive value (PPV), and NPV were calculated to predict the ability of each modality to identify hemodynamically significant stenoses on both a per-vessel and per-patient basis. Interobserver variability was compared using kappa statistic values and Bland-Altman plots for visual perfusion assessment and transmural perfusion ratio. Given that coronary CTA and visual perfusion assessment were performed together to reflect recommended clinical practice, the incremental value of visual perfusion assessment over and above the coronary CTA analysis was evaluated by creating a coronary CTA–visual perfusion assessment interaction term. The associations between FFR ≤0.8, coronary CTA, the transmural perfusion ratio, coronary CTA ▫ transmural perfusion ratio, and coronary CTA ▫ visual perfusion assessment were evaluated using a generalized estimating equation approach. Patient identity was included as a cluster variable to account for likely within-individual correlations, given that evaluation of multiple arteries was made from each individual. FFR as a dichotomous variable was assumed to have a binomial probability distribution, which is supported by existing literature from a similar patient cohort (2-sided binomial probability test, p ▫ 0.9) (16). To examine the association between covariates of interest and continuous variables, mixed-effects modeling was performed with patient identity included as a random effect to account for the fact that multiple arteries were examined in each participant.

Receiver-operating characteristic (ROC) curve analysis was undertaken to evaluate the discriminatory ability of coronary CTA, the transmural perfusion ratio, coronary CTA ▫ visual perfusion assessment, and coronary CTA ▫ the transmural perfusion ratio for FFR ≤0.8. The optimal transmural perfusion ratio threshold that provided at least 70% sensitivity and maximized the sum of

Table 2. CT Scan Parameters

	Coronary CTA	CTP
Heart rate (beats/min)*	53.8 ▫ 7.4	68.4 ▫ 8.9
Beta-blocker use	37 (93)	
Oral metoprolol	37 (93)	
Intravenous metoprolol	19 (48)	
Beta-blocker dose, mg		
Oral metoprolol	58 ▫ 31	
Intravenous metoprolol	6 ▫ 11	
Gantry rotations*		
1	36 (90)	22 (55)
2	4 (10)	18 (45)
Tube voltage, kV	120 ▫ 0	120 ▫ 0
Tube current, mA	483 ▫ 58	423 ▫ 60
Dose length product, mGy/cm	379 ▫ 157	343 ▫ 186
Radiation exposure, mSv	4.7 ▫ 3.9	4.5 ▫ 1.9

Values are mean ▫ SD or n (%). *At time of CT image acquisition.
CT ▫ computed tomography; CTA ▫ computed tomography angiography; CTP ▫ computed tomography stress myocardial perfusion imaging.

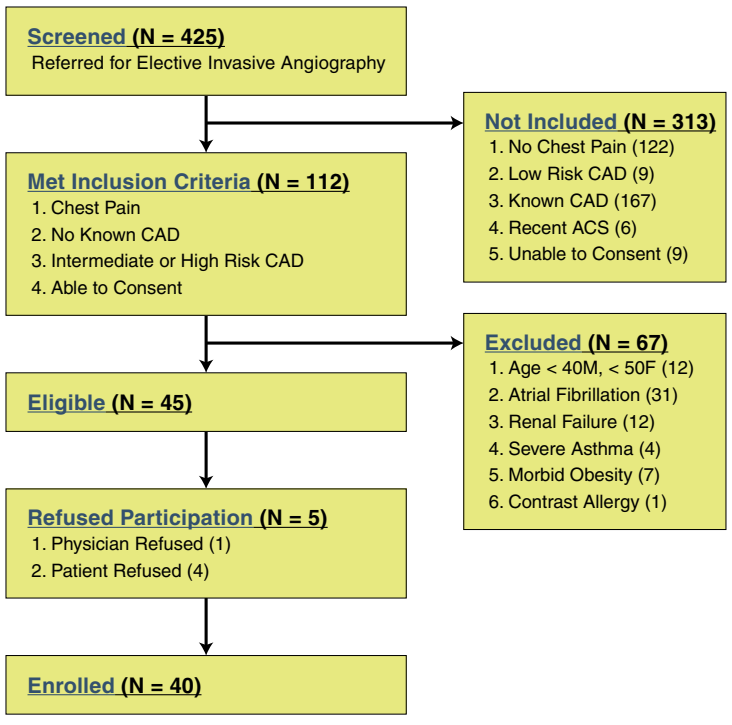

Figure 2. Patient Flow Diagram

A total of 112 patients were screened and met inclusion criteria; 67 were excluded. Forty patients were enrolled and completed the entire protocol. ACS ▫ acute coronary syndromes; CAD ▫ coronary artery disease.

sensitivity and specificity for FFR ≤0.8 was determined. Areas under the ROC curves were compared using the approach of DeLong et al. (17) with Bonferroni adjustment for pairwise comparisons. To evaluate the incremental discriminatory ability of transmural perfusion ratio and/or visual perfusion assessment over and above the coronary CTA assessment of stenosis, the integrated discrimination improvement (IDI) index was used, as described by Pencina et al. (18). An IDI index that is significantly greater than zero is taken to demonstrate the incremental value of the novel perfusion imaging technique when added to coronary CTA. Statistical analysis was performed with STATA 12.1 (StataCorp, College Station, Texas). A threshold of α ▫ 0.05 was adopted to demonstrate statistical significance.

RESULTS

Patient population. Forty patients (mean age 61.5 ▫ 9.9 years; 67.5% male) were enrolled and successfully underwent CT protocol and FFR assessment. Subject characteristics and CT scan parameters are summarized in Tables 1 and 2, respectively. The patient flow chart is illustrated in Figure 2.

Seventy-seven major vessels (64.2%) were successfully interrogated by FFR. FFR was assumed in the remaining 43 vessels, of which 22 were angiographically smooth or had minor irregularities and 21 had stenoses ▫ 90%.

Twenty-three of 40 patients had stenoses ≥50% in at least 1 coronary artery on quantitative coronary angiography. FFR-significant stenoses were present in 21 patients (52.5%), of whom 9 (22.5%) had single-vessel disease, 5 (12.5%) had 2-vessel disease, and 7 (17.5%) had 3-vessel disease. Overall, 40 of 120 vessels (33.3%) had FFR-significant disease.

The diagnostic accuracy of coronary CTA interpretation alone and combined coronary CTA and CTP interpretation in the detection of hemodynamically significant stenoses is summarized in Figures 3 and 4 and Tables 3 and 4. An example is illustrated in Figure 5.

Coronary CTA. Coronary CTA alone had a per-vessel sensitivity for FFR-significant stenoses of 95%, a specificity of 78%, a PPV of 68%, an NPV of 97%, and an accuracy of 83%. The corresponding numbers for per-patient analysis were 95%, 68%, 77%, 93%, and 83%, respectively.

CTP assessment. Due to the presence of artifacts, qualitative assessment and the transmural perfusion ratio were not interpretable in 3 and 17 vessels, respectively, which were excluded from analysis.

On visual inspection, 39 vessels had stress perfusion defects, 38 defects were reversible, and 8 were transmural. Of the 39 vessels, 34 (87%) contained FFR-significant stenoses, whereas the remaining 5 (2 in the left anterior descending artery [LAD], 2 in the left circumflex artery [LCx], and 1 in the right coronary artery [RCA]) were not FFR significant. In the remaining 78 vessels assessed to have normal perfusion, 73 (94%) were not FFR significant. Five vessels (6%) (3 RCA, 2 LAD) were significant on FFR (FFR range 0.75 to 0.80). There was good interobserver and intraobserver agreement with a kappa value of 0.72 (95% confidence interval [CI]: 0.41 to 1.00) and 0.67 (95% CI: 0.37 to 0.97), respectively. Image quality was graded moderate, good, or excellent in 87% (104 of 120) of vessels. Mean reader confidence was 1.58 ▫ 1.02.

On quantitative perfusion analysis, 50 vessels had a transmural perfusion ratio value ▫ 0.99, and 28 (56%) contained FFR-significant stenoses. In the remaining 53 vessels that had a transmural perfusion ratio value ≥0.99, 43 (81%) were not significant on FFR. In the intraobserver analysis, the 95% limit of agreement was between ▫ 7.9% and 11.7%,

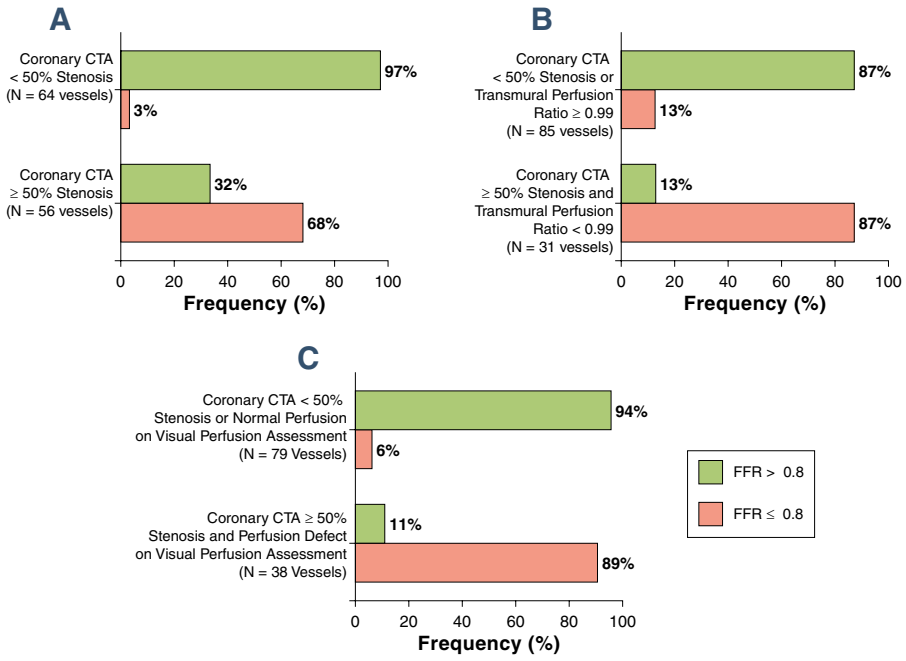

Figure 3. Relationship Between Coronary CTA, Coronary CTA + Transmural Perfusion Ratio, and Coronary CTA + Visual Perfusion Assessment Versus FFR

The positive and negative predictive values of coronary CTA for fractional flow reserve (FFR)–significant stenosis were 68% and 97%, respectively **(A)**. By adding the transmural perfusion ratio and visual perfusion assessment to coronary CTA interpretation, the positive predictive value increased to 87% and 89%, respectively, and the negative predictive value decreased to 87% and 94%, respectively **(B, C)**. Abbreviations as in Figure 1.

with a 1.9% bias. In the interobserver analysis, the 95% limit of agreement was between □ 18.5% and 15.8%, with a □ 1.4% bias.

The transmural perfusion ratio was significantly associated with FFR ≤0.8, using generalized estimating equation modeling (p □ 0.001). This association was independent of the presence of significant coronary CTA stenosis using mixed-effects modeling (p □ 0.001). The mean transmural perfusion ratio in FFR-significant vessels was significantly lower compared with nonsignificant vessels (0.91 □ 0.10 vs. 0.98 □ 0.08, p □ 0.001) (Fig. 4A). On ROC analysis, the area under the curve (AUC) for transmural perfusion ratio was 0.76 (95% CI: 0.66 to 0.86, p □ 0.0001). Compared with coronary CTA, the transmural perfusion ratio alone was not demonstrated to be superior for the identification of FFR significant stenoses (coronary CTA AUC: 0.85; 95% CI: 0.79 to 0.91). In fact, there was a trend toward a greater AUC for coronary CTA (p □ 0.07).

A transmural perfusion ratio threshold of □ 0.99 provided at least 70% sensitivity and optimized the sum of sensitivity and specificity (Fig. 4B). Overall, a transmural perfusion ratio threshold □ 0.99 predicted hemodynamically significant stenoses with 74% sensitivity, 66% specificity, 56% PPV, 81% NPV, and 69% accuracy.

Combined coronary CTA and visual perfusion interpretation. The presence of ≥50% stenosis on coronary CTA and a stress perfusion defect significantly increased the per-vessel specificity to 95%, the PPV to 89%, and overall accuracy to 92% compared with coronary CTA alone. Sensitivity was 87% and NPV was 94%. In the presence of ≥50% stenosis on coronary CTA, 89% of vessels identified with a perfusion defect contained FFR-significant stenoses, whereas 80% of vessels identified to have normal perfusion had no FFR-significant disease. In the absence of ≥50% stenosis on CT, the majority of vessels had normal CT perfusion (98%) and nonsignificant FFR (97%) (Fig. 6).

Combined coronary CTA and transmural perfusion ratio interpretation. Despite an uninterpretable transmural perfusion ratio in 17 vessels, 13 were subtended by □ 50% stenoses on coronary CTA and were included in the coronary CTA □ transmural perfusion ratio analysis. The presence of ≥50% stenosis on coronary CTA and a transmural perfusion ratio

JACC: CARDIOVASCULAR IMAGING, VOL. 5, NO. 11, 2012
NOVEMBER 2012:1097–111

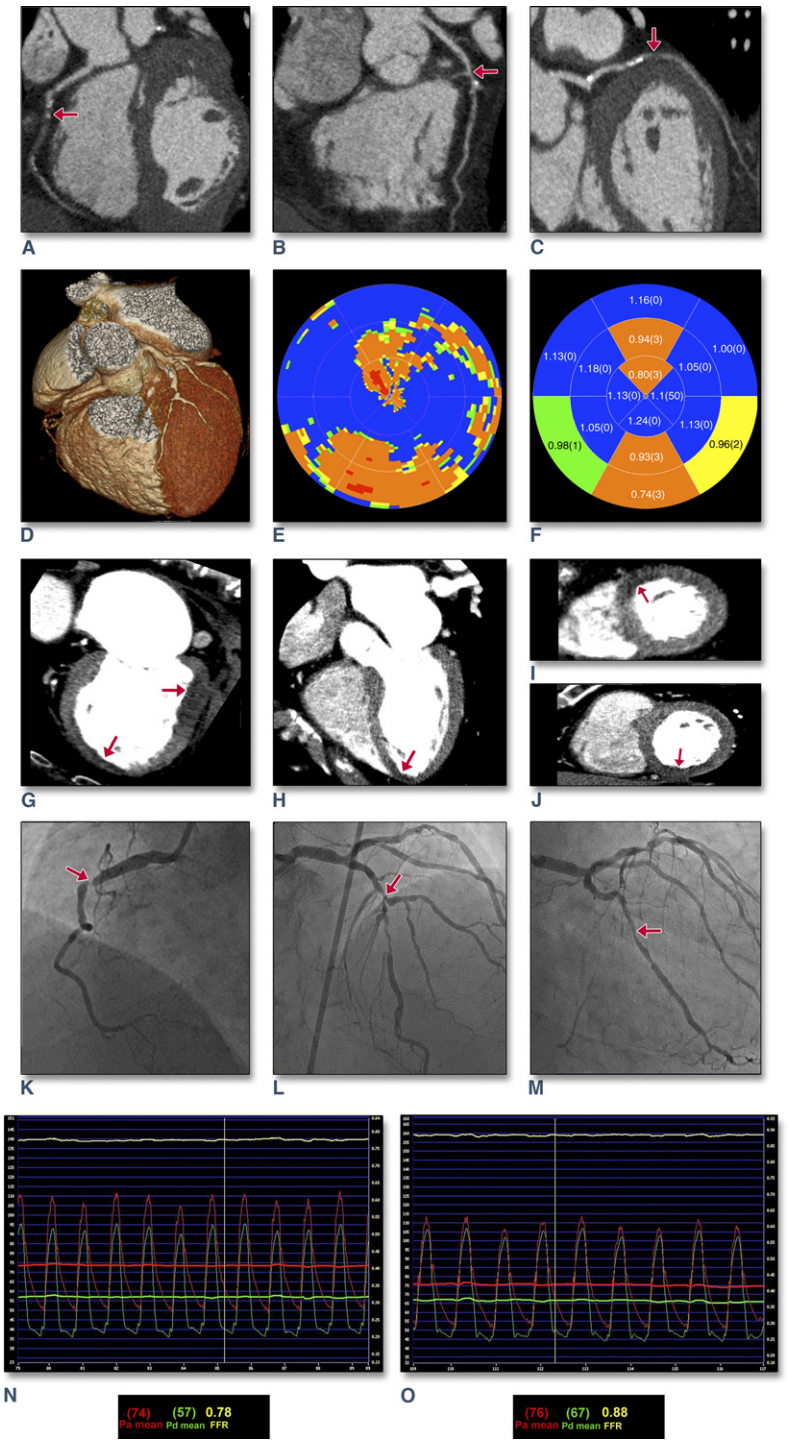

Figure 4. Example of Combined Coronary CTA + CTP and ICA + FFR

A 69-year-old woman with chest pain and suspected coronary artery disease. Coronary CTA demonstrated severe stenosis in the left anterior descending artery (LAD) and left circumflex (LCx) and a chronic total occlusion of the right coronary artery (RCA) **(A, B, C, D)**. Polar plot for the transmural perfusion ratio demonstrates moderate ischemia **(orange)** in the mid and distal anterior and basal and mid inferior walls and normal perfusion in the remaining walls **(blue) (E)**. Transmural perfusion ratios in the LAD, RCA, and LCX were 0.82, 0.75, and 1.01, respectively **(F)**. Visual perfusion assessment identified perfusion defects in the mid and distal anterior segments, which indicated LAD ischemia, and in the basal and mid inferior segments extending into the basal inferolateral segment, which indicated RCA ischemia **(G, H, I, J)**. Invasive coronary angiography confirmed severe stenoses in the LAD and LCx and chronic total occlusion of the RCA **(K, L, M)**. The right posterior descending artery and right posterolateral branches filled retrogradely from the LAD and LCx, respectively. The FFR was 0.77 in the LAD, 0.88 in the LCx, and assumed to be 0.5 in the RCA **(N, O)**. Abbreviations as in Figures 1 and 3.

Table 3. Per-Vessel Territory Diagnostic Accuracy of Coronary CTA, Coronary CTA + Transmural Perfusion Ratio, Coronary CTA + Visual Perfusion Assessment Compared With FFR

	Coronary CTA ≥50% (n = 120)	Transmural Perfusion Ratio <0.99 (n = 103)	Coronary CTA ≥50% and Transmural Perfusion Ratio <0.99 (n = 116)	Coronary CTA ≥50% and Perfusion Defect on Visual Perfusion Assessment (n = 118)
True positive	38	28	27	34
False positive	18	22	4	4
True negative	62	43	74	75
False negative	2	10	11	5
Sensitivity	95 (82–99)	74 (57–86)	71 (64–84)	87 (72–95)
Specificity	78 (67–86)	66 (53–77)	95 (87–98)	95 (87–98)
PPV	68 (54–79)	56 (41–70)	87 (69–96)	89 (74–97)
NPV	97 (88–100)	81 (68–90)	87 (78–93)	94 (85–98)
Kappa statistic	0.66 (0.52–0.80)	0.37 (0.19–0.55)	0.69 (0.55–0.84)	0.83 (0.72–0.94)
Accuracy, %	83	69	87	92
AUC on ROC	0.85* (0.78–0.91)	0.76* (0.66–0.86)	0.79* (0.69–0.88)	0.93* (0.87–0.98)
IDI	—	—	0.05†	0.22‡

Values are n or % (95% CI). *p ▫ 0.0001. †p ▫ 0.0001. ‡p ▫ 0.02.
AUC ▫ area under the curve; CI ▫ confidence interval; CTA ▫ computed tomography angiography; FFR ▫ fractional flow reserve; IDI ▫ integrated discrimination improvement; NPV ▫ negative predictive value; PPV ▫ positive predictive value; ROC ▫ receiver-operating characteristic.

▫ 0.99 increased the per-vessel specificity to 95% and the PPV to 87% compared with coronary CTA alone. Sensitivity and the NPV decreased to 71% and 87%, respectively. There were 11 false-negative vessels, 6 of which occurred in the LAD (3 in LCx, 2 in RCA). Overall accuracy increased to 87%. In the presence of ≥50% stenosis on coronary CTA, 87% of vessels with an abnormal transmural perfusion ratio contained FFR-significant stenoses, whereas only 57% of vessels with a normal transmural perfusion ratio were found to be nonsignificant on FFR (Fig. 7). In the absence of ≥50% stenosis on CT, only 50% were identified to have a normal transmural perfusion ratio.

Incremental value of visual perfusion assessment and transmural perfusion ratio on coronary CTA. Visual perfusion assessment provided superior incremental value when used in combination with coronary CTA compared with transmural perfusion ratio (Table 3, Fig. 8). On ROC analysis, the AUC for coronary CTA ▫ visual perfusion assessment was significantly greater than the AUCs for coronary CTA alone (0.93 vs. 0.85, p ▫ 0.0003), transmural perfusion ratio (0.93 vs. 0.76, p ▫ 0.0001), and coronary CTA ▫ transmural perfusion ratio (0.93 vs. 0.79, p ▫ 0.0003).

The results of the IDI index confirmed the ROC findings. When added to coronary CTA, visual perfusion assessment provided significant incremental value (IDI ▫ 0.22, p ▫ 0.0001) for identifying FFR-significant stenoses. In contrast, there was only modest incremental value when the transmural perfusion ratio was added to coronary CTA (IDI ▫ 0.054, p ▫ 0.02) for identifying FFR-significant stenoses.

Table 4. Per-Patient Territory Diagnostic Accuracy of Coronary CTA, Coronary CTA + Transmural Perfusion Ratio, Coronary CTA + Visual Perfusion Assessment Compared With FFR

	Coronary CTA ≥50% (n = 40)	Transmural Perfusion Ratio <0.99 (n = 28)	Coronary CTA ≥50% and Transmural Perfusion Ratio <0.99 (n = 38)	Coronary CTA ≥50% and Perfusion Defect on Visual Perfusion Assessment (n = 39)
True positive	20	18	18	19
False positive	6	6	2	1
True negative	13	4	17	18
False negative	1	0	1	1
Sensitivity	95 (74–100)	100 (78–100)	95 (72–100)	95 (73–100)
Specificity	68 (44–86)	40 (14–73)	90 (66–98)	95 (72–100)
PPV	77 (56–90)	75 (63–89)	90 (67–98)	95 (73–100)
NPV	93 (64–100)	100 (40–100)	94 (71–100)	95 (72–100)
Kappa statistic	0.64 (0.41–0.88)	0.46 (0.08–0.84)	0.84 (0.67–1.0)	0.90 (0.76–1.0)
Accuracy, %	83	79	92	95

Values are n or % (95% CI).
Abbreviations as in Table 3.

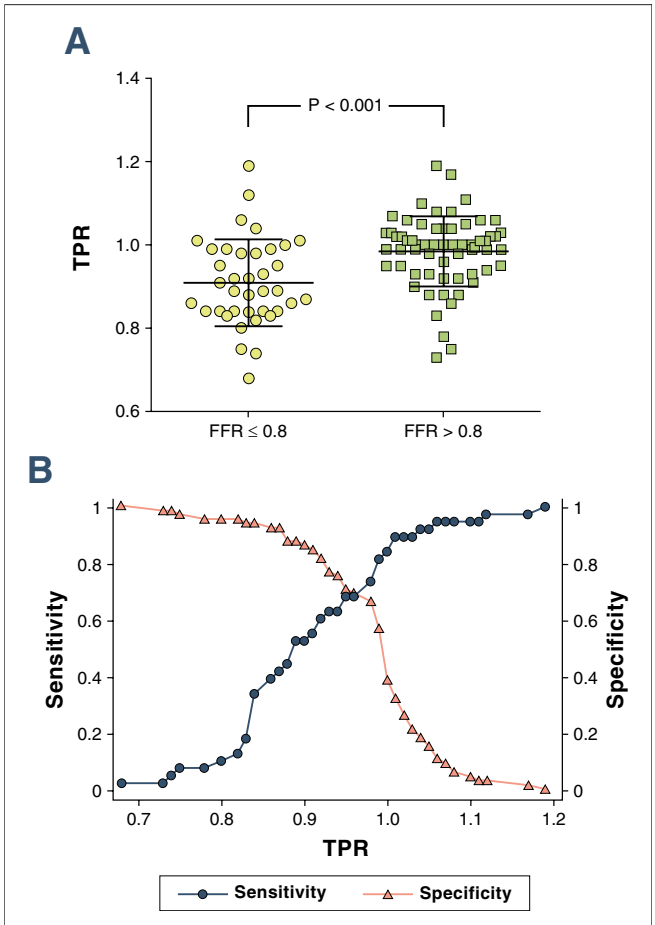

Figure 5. Relationship Between Transmural Perfusion Ratio and FFR

(A) The mean TPR in FFR-significant vessels was significantly lower compared with nonsignificant vessels (0.91 ▫ 0.10 vs. 0.98 ▫ 0.08, p ▫ 0.001). **(B)** The TPR threshold that provided at least 70% sensitivity and yielded the maximum sum of sensitivity and specificity on the receiver-operating characteristic curve was ▫ 0.99. This provided 76% sensitivity and 66% specificity. Abbreviations as in Figures 1 and 3.

Duration of CT protocol and radiation dose. The mean radiation dose for rest coronary CTA was 4.7 ▫ 3.2 mSv, 4.5 ▫ 1.8 mSv for the stress perfusion scan, and 9.2 ▫ 3.5 mSv for the entire CT protocol. The average duration required to perform the entire CT protocol was 42.6 ▫ 5.6 min. The average duration spent in the CT department, including time before and after the scans, was 159.6 ▫ 30.8 min.

DISCUSSION

This study is the first to report on the incremental value of 320-row detector CTP when used in addition to coronary CTA to detect hemodynamically significant stenoses in symptomatic patients with suspected CAD. It is also the first to compare the added accuracy of quantitative and qualitative CT perfusion assessment.

We demonstrate that the additional use of CTP significantly increases the ability of coronary CTA to detect hemodynamically significant stenoses. Both qualitative and quantitative perfusion assessment significantly increases specificity and hence accuracy. The additional use of expert visual perfusion assessment compared with the transmural perfusion ratio provides superior sensitivity and overall accuracy, which is confirmed by the significant incremental value determined on ROC AUC and IDI analyses. Combined coronary CTA and CTP, when interpreted in the same setting, provides excellent per-patient accuracy ▫ 90% compared with FFR, and this can be achieved with a short CT performance duration and an acceptable radiation dose.

Past studies predominantly evaluated the accuracy of CT perfusion in known CAD (3,4,19,20). In practice, these patients are unlikely to be referred for coronary CTA. This study evaluates the role of coronary CTA ▫ CTP in intermediate-risk patients for whom coronary CTA is deemed appropriate (5) and cardiac CT use is predicted to increase (21) and in high-risk patients who would otherwise be referred for noninvasive functional testing (22). The rest followed by a stress study CT protocol provided an opportunity to evaluate whether the combined CT protocol can be terminated if minimal disease only is identified on the rest coronary CTA. Our results support the performance of coronary CTA alone in the absence of ≥50% stenosis, a finding that excluded FFR-significant stenoses with an NPV of 97%, in keeping with previous studies reporting an NPV ranging from 90% to 100% (2–4,16). A potential disadvantage in the ordering sequence is the possibility of late contrast enhancement from the rest study during stress imaging. This can be minimized by ensuring at least a 20-min interval between scans (23).

We believe that this is the first study to report the accuracy of combined interpretation of 320-row detector coronary CTA and CTP to detect hemodynamically significant stenoses. Our findings confirm the high accuracy of combined coronary CTA ▫ CTP interpretation compared with coronary CTA alone to detect hemodynamically significant stenoses and extend the work of Rocha-Filho et al. (24), who demonstrated that combined dual-source coronary CTA and CTP interpretation improved the diagnostic accuracy of coronary CTA for detecting

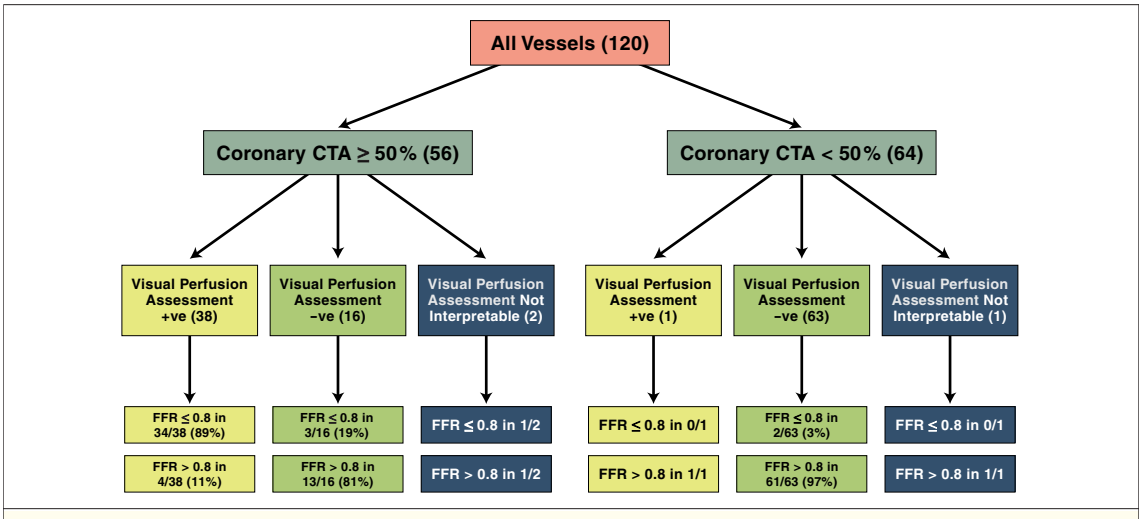

Figure 6. Algorithm Illustrating the Use of Sequential Coronary CTA and Visual Perfusion Assessment on CT

In the presence of ≥50% stenosis on CT, 89% of vessels identified with a perfusion defect were found to contain FFR-significant stenoses, whereas 80% of vessels identified having normal perfusion were found to have no significant disease on FFR. In the absence of ≥50% stenosis on CT, the vast majority of vessels had normal CT perfusion (98%) and nonsignificant FFR (97%). ▫ve ▫ positive; ▫ve ▫ negative; other abbreviations as in Figures 1 and 3.

anatomically occlusive CAD. A similar method is currently used in positron emission tomography/CT cardiac hybrid imaging interpretation and has significantly enhanced accuracy, particularly in multivessel disease and reader confidence (25,26). ROC analysis indicates that the use of a transmural perfusion ratio threshold ▫ 0.99 provides the highest sensitivity (74%) and specificity (66%) for the detection of hemodynamically significant stenoses. However, this implies that there remains a significant overlap in transmural perfusion ratio values of vessels with and without FFR-significant stenoses. George et al. (7) recommended the use of the same transmural perfusion ratio threshold based on quantitative coronary angiography and reported a per-vessel sensitivity of 70% and specificity of 51% when the transmural perfusion ratio was compared with single-photon emission CT perfusion alone.

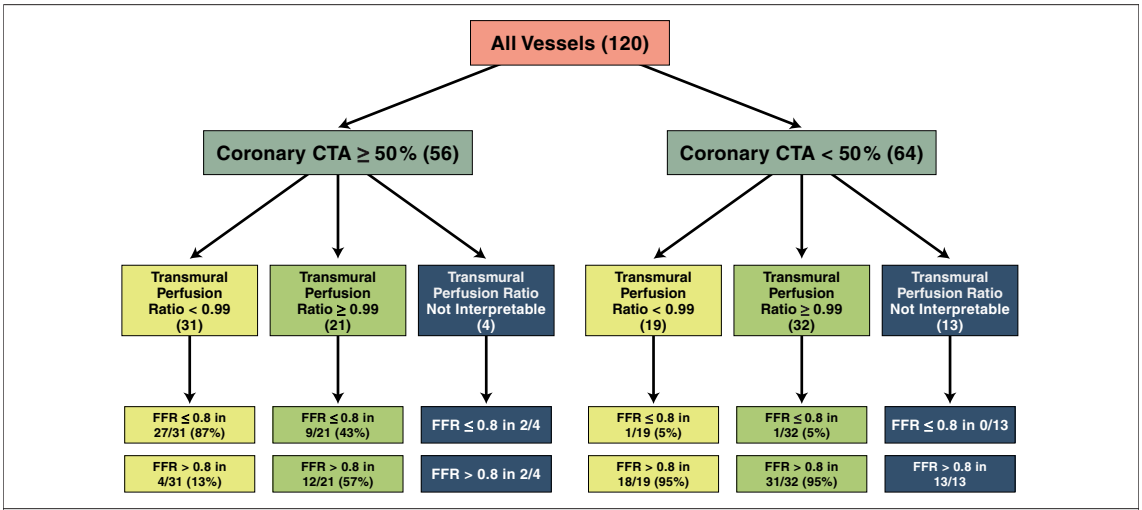

Figure 7. Algorithm Illustrating the Use of Sequential Coronary CTA and Quantitative Perfusion Assessment Using the TPR

In the presence of ≥50% stenosis on CT, 87% of vessels with an abnormal transmural perfusion ratio were found to contain FFR-significant stenoses, whereas 57% of vessels with a normal transmural perfusion ratio were found to be nonsignificant on FFR. In the absence of ≥50% stenosis on CT, 50% were identified as having a normal transmural perfusion ratio. ▫ve ▫ positive; ▫ve ▫ negative; other abbreviations as in Figures 1 and 3.

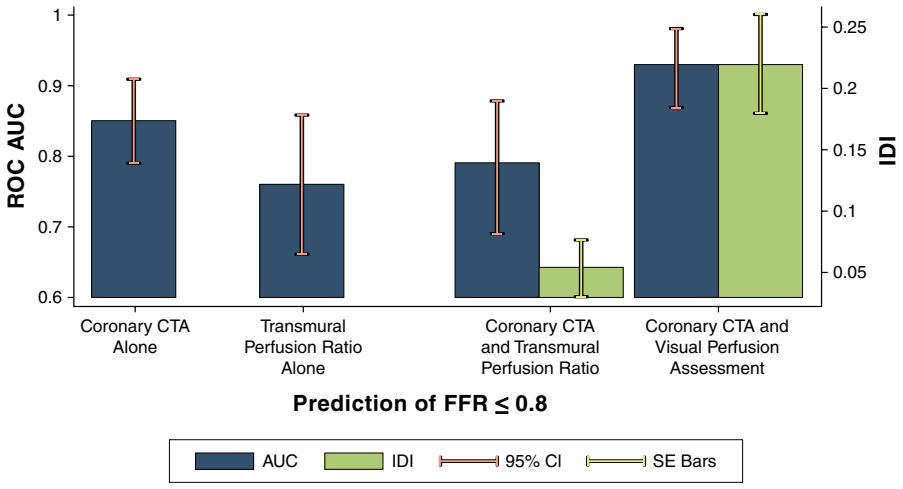

Figure 8. Incremental Value of TPR and VPA When Added to Coronary CTA to Detect FFR-Significant Stenoses

Area under the curve (AUC) for coronary CTA ▫ VPA was significantly greater than the AUCs for coronary CTA alone (0.93 vs. 0.85, p ▫ 0.0003), TPR (0.93 vs. 0.76, p ▫ 0.0001), and coronary CTA ▫ TPR (0.93 vs. 0.79, p ▫ 0.0003). The integrated discrimination improvement (IDI) demonstrated incremental benefit of both TPR (0.05, SE ▫ 0.02, p ▫ 0.02) and VPA (0.02, SE ▫ 0.04; p ▫ 0.0001) when added to coronary CTA. CI ▫ confidence interval; other abbreviations as in Figures 1 and 3.

When used with coronary CTA, visual perfusion assessment provided higher sensitivity and overall accuracy than the transmural perfusion ratio. These findings are indeed supported by the superior incremental value of visual perfusion assessment as indicated by the IDI and ROC AUC analyses.

The main difference in the 2 techniques may be explained by a higher number of false-negative vessels when the transmural perfusion ratio is used compared with visual perfusion assessment (11 vs. 4 vessels). The majority of these vessels (8 of 11) occurred in 5 patients in whom all 3 vessels had FFR-significant stenoses, thereby raising the possibility that balanced ischemia may result in a false normalization of the transmural perfusion ratio in these circumstances.

An explanation for the lower NPV with quantitative assessment may be the mathematical derivation of the transmural perfusion ratio as the ratio of subendocardial and subepicardial contrast attenuation. Subendocardial attenuation represents segment-specific subendocardial attenuation, and subepicardial attenuation is derived from the mean attenuation of the entire subepicardial layer of any given short-axis slice. This approach aims to provide accurate transmural perfusion ratio assessment despite the potential presence of transmural ischemia in any given segment. In the presence of balanced transmural ischemia across an entire short-axis slice, both subendocardial and subepicardial attenuation are decreased; thus, the ratio may be falsely normalized. In contrast, the CT angiographer during qualitative assessment has the ability to scroll between and compare various short-axis slices, which may improve the ability to correctly identify the presence of balanced transmural ischemia inherent across a particular short-axis slice.

Our results extend the work of Bamberg et al. (4), who demonstrated that myocardial blood flow determined by dynamic CT using second-generation dual-source cardiac CT increased the overall accuracy of coronary CTA alone in the detection of FFR-significant stenoses. Combined use of coronary CTA ▫ MBF had 93% sensitivity and 87% specificity, which is similar to our results. Notably, we used "static" imaging acquired during the first pass of contrast with a 320-row CT scanner and prospective electrocardiographic gating, which is associated with a reduced radiation dose (4.5 mSv vs. 10 mSv for perfusion assessment).

Currently, many patients who have ≥50% stenosis on coronary CTA are either referred for ICA or for a noninvasive functional test. Such a policy will invariably result in a large number of unnecessary referrals for ICA, which has a limited inherent accuracy in the detection of hemodynamically significant stenoses (27,28). Yet the accuracy to detect FFR-significant stenoses remains low for commonly available functional tests including stress echocardiography and single-photon emission CT (29,30).

Our work supports the use of cardiac CT as a "one-stop shop" to evaluate both coronary anatomy and perfusion in suspected CAD. Using this technique, there is a decrease in the number of patients with false-positive results (coronary CTA □ visual perfusion assessment [n □ 1] vs. coronary CTA [n □ 6]), which was demonstrated by a significant increase in per-patient specificity (coronary CTA □ visual perfusion assessment, 95% vs. coronary CTA, 68%). These results require further confirmation from results of large multicenter studies including the CORE 320 (Combined Non-invasive Coronary Angiography and Myocardial Perfusion Imaging Using 320 Detector Computed Tomography) trial and Regadenoson Crossover (A Study of Regadenoson in Subjects Undergoing Stress Myocardial Perfusion Imaging [MPI] Using Multidetector Computed Tomography [MDCT] Compared to Single Photon Emission Computed Tomography [SPECT]) trial and ultimately multicenter studies that use the FFR as a reference standard.

Recently, noninvasive FFR computed using CT has been demonstrated to be moderately accurate in the detection of FFR significant stenoses (31,32). An advantage over CTP is that hemodynamic data can be derived from resting coronary CTA without the need for an additional stress scan, hence, the added convenience and lower radiation. However, its computation is dependent on the use of a supercomputer and coronary CTA image quality. Future comparative studies may be required to determine their ultimate role in suspected CAD.

Study limitations. Although the largest study thus far reported in symptomatic patients with suspected CAD, our results represent a single-center study with limited patient numbers. Second, we did not perform delayed contrast-enhanced imaging in this imaging protocol; thus, we could not delineate any effect of previous infarction on the accuracy of cardiac CTP. Third, the FFR was only measured in 64% of arteries; however, in noninterrogated arteries, the assumptions made for occluded and normal arteries were as per standard assumptions in other published studies (14,33). Furthermore, the coronary CTA □ CTP findings were compared with FFR alone without taking into account microvascular disease. Fourth, beta-blockers were given before the perfusion scan in 93% of patients. Although this may decrease the sensitivity for ischemia in exercise stress imaging, this has not been observed in adenosine stress imaging (34). Last, because combined coronary CTA □ CTP requires a double iodinated contrast dose (120 ml) compared with coronary CTA alone, it needs to be used with caution in patients with abnormal renal function.

CONCLUSIONS

In patients with suspected CAD, combined coronary CTA and CTP imaging and single-setting interpretation provide excellent accuracy in the detection of patients with hemodynamically significant stenoses compared with FFR. The additional use of both qualitative and quantitative CTP assessment with coronary CTA significantly improved the specificity and overall accuracy of coronary CTA, whereas visual perfusion assessment provided superior sensitivity and incremental value compared with the transmural perfusion ratio. The combined coronary CTA and CTP imaging protocol is achieved using an acceptable radiation dose and has a short CT performance duration. This work supports the use of cardiac CT as a "one-stop shop" to accurately and conveniently evaluate both coronary anatomy and myocardial perfusion in the future diagnostic evaluation of symptomatic patients with suspected CAD. Table 2.

Acknowledgments

The authors express their gratitude to Dennis Wong for assistance in preparation of this manuscript and to the MonashHeart catheterization laboratory staff for technical support.

Reprint requests and correspondence: Dr. Sujith K. Seneviratne, MonashHeart, 246 Clayton Road, Clayton, 3168 Victoria, Australia. *E-mail: Sujith.Seneviratne@southernhealth.org.au.*

REFERENCES

1. Budoff MJ, Dowe D, Jollis JG, et al. Diagnostic performance of 64-multidetector row coronary computed tomographic angiography for evaluation of coronary artery stenosis in individuals without known coronary artery disease: results from the prospective multicenter ACCURACY (Assessment by Coronary Computed Tomographic Angiography of Individuals Undergoing Invasive Coronary Angiography) trial. J Am Coll Cardiol 2008;52:1724–32.
2. Meijboom WB, Van Mieghem CA, van Pelt N, et al. Comprehensive assessment of coronary artery stenoses: computed tomography coronary angiography versus conventional coronary angiography and correlation with fractional flow reserve in patients with stable angina. J Am Coll Cardiol 2008;52:636–43.
3. Ko BS, Cameron JD, Meredith IT, et al. Computed tomography stress myocardial perfusion imaging in patients considered for revascularization: a comparison with fractional flow reserve. Eur Heart J 2012; 33:67–77.

4. Bamberg F, Becker A, Schwarz F, et al. Detection of hemodynamically significant coronary artery stenosis: incremental diagnostic value of dynamic CT-based myocardial perfusion imaging. Radiology 2011;260:689–98.
5. Taylor AJ, Cerqueira M, Hodgson JM, et al. ACCF/SCCT/ACR/AHA/ASE/ASNC/NASCI/SCAI/SCMR 2010 appropriate use criteria for cardiac computed tomography. A report of the American College of Cardiology Foundation Appropriate Use Criteria Task Force, the Society of Cardiovascular Computed Tomography, the American College of Radiology, the American Heart Association, the American Society of Echocardiography, the American Society of Nuclear Cardiology, the North American Society for Cardiovascular Imaging, the Society for Cardiovascular Angiography and Interventions, and the Society for Cardiovascular Magnetic Resonance. J Am Coll Cardiol 2010; 56:1864–94.
6. Mehra VC, Valdiviezo C, Arbab-Zadeh A, et al. A stepwise approach to the visual interpretation of CT-based myocardial perfusion. J Cardiovasc Comput Tomogr 2011;5:357–69.
7. George RT, Arbab-Zadeh A, Miller JM, et al. Adenosine stress 64- and 256-row detector computed tomography angiography and perfusion imaging: a pilot study evaluating the transmural extent of perfusion abnormalities to predict atherosclerosis causing myocardial ischemia. Circ Cardiovasc Imaging 2009;2:174–82.
8. Blankstein R, Shturman LD, Rogers IS, et al. Adenosine-induced stress myocardial perfusion imaging using dual-source cardiac computed tomography. J Am Coll Cardiol 2009;54: 1072–84.
9. Diamond GA, Forrester JS. Analysis of probability as an aid in the clinical diagnosis of coronary-artery disease. N Engl J Med 1979;300:1350–8.
10. Gibbons RJ, Chatterjee K, Daley J, et al. ACC/AHA/ACP-ASIM guidelines for the management of patients with chronic stable angina. A report of the American College of Cardiology/American Heart Association Task Force on Practice Guidelines (Committee on Management of Patients with Chronic Stable Angina). J Am Coll Cardiol 1999;33:2092–197.
11. Hausleiter J, Meyer T, Hermann F, et al. Estimated radiation dose associated with cardiac CT angiography. JAMA 2009;301:500–7.
12. Sianos G, Morel MA, Kappetein AP, et al. The SYNTAX Score: an angiographic tool grading the complexity of coronary artery disease. EuroIntervention 2005;1:219–27.
13. Cerqueira MD, Weissman NJ, Dilsizian V, et al. Standardized myocardial segmentation and nomenclature for tomographic imaging of the heart: a statement for healthcare professionals from the Cardiac Imaging Committee of the Council on Clinical Cardiology of the American Heart Association. J Nucl Cardiol 2002;9:240–5.
14. Melikian N, De Bondt P, Tonino P, et al. Fractional flow reserve and myocardial perfusion imaging in patients with angiographic multivessel coronary artery disease. J Am Coll Cardiol Intv 2010;3:307–14.
15. Tonino PA, De Bruyne B, Pijls NH, et al. Fractional flow reserve versus angiography for guiding percutaneous coronary intervention. N Engl J Med 2009;360:213–24.
16. Kajander S, Joutsiniemi E, Saraste M, et al. Cardiac positron emission tomography/computed tomography imaging accurately detects anatomically and functionally significant coronary artery disease. Circulation 2010;122: 603–13.
17. Delong ML, Duncan BD, Parker JH. Parametric extension of the classical exposure-schedule theory for angle-multiplexed photorefractive recording over wide angles. Appl Opt 1998;37: 3015–30.
18. Pencina MJ, D'Agostino RB Sr., D'Agostino RB Jr., Vasan RS. Evaluating the added predictive ability of a new marker: from area under the ROC curve to reclassification and beyond. Stat Med 2008;27:157–72; discussion 207–12.
19. Feuchtner G, Goetti R, Plass A, et al. Adenosine stress high-pitch 128-slice dual-source myocardial computed tomography perfusion for imaging of reversible myocardial ischemia: comparison with magnetic resonance imaging. Circ Cardiovasc Imaging 2011; 4:540–9.
20. Bastarrika G, Ramos-Duran L, Rosenblum MA, Kang DK, Rowe GW, Schoepf UJ. Adenosine-stress dynamic myocardial CT perfusion imaging: initial clinical experience. Invest Radiol 2010;45:306–13.
21. Shaw LJ, Marwick TH, Zoghbi WA, et al. Why all the focus on cardiac imaging? J Am Coll Cardiol Img 2010;3:789–94.
22. Hendel RC, Berman DS, Di Carli MF, et al., American College of Cardiology Foundation Appropriate Use Criteria Task Force; American Society of Nuclear Cardiology; American College of Radiology; American Heart Association; American Society of Echocardiology; Society of Cardiovascular Computed Tomography; Society for Cardiovascular Magnetic Resonance; Society of Nuclear Medicine. ACCF/ASNC/ACR/AHA/ASE/SCCT/SCMR/SNM 2009 appropriate use criteria for cardiac radionuclide imaging: a report of the American College of Cardiology Foundation Appropriate Use Criteria Task Force, the American Society of Nuclear Cardiology, the American College of Radiology, the American Heart Association, the American Society of Echocardiography, the Society of Cardiovascular Computed Tomography, the Society for Cardiovascular Magnetic Resonance, and the Society of Nuclear Medicine. J Am Coll Cardiol 2009;53:2201–29.
23. Techasith T, Cury RC. Stress myocardial CT perfusion: an update and future perspective. J Am Coll Cardiol Img 2011;4:905–16.
24. Rocha-Filho JA, Blankstein R, Shturman LD, et al. Incremental value of adenosine-induced stress myocardial perfusion imaging with dual-source CT at cardiac CT angiography. Radiology 2010;254:410–9.
25. Flotats A, Knuuti J, Gutberlet M, et al. Hybrid cardiac imaging: SPECT/CT and PET/CT. A joint position statement by the European Association of Nuclear Medicine (EANM), the European Society of Cardiac Radiology (ESCR) and the European Council of Nuclear Cardiology (ECNC). Eur J Nucl Med Mol Imaging 2011;38: 201–12.
26. Pazhenkottil AP, Nkoulou RN, Ghadri JR, et al. Prognostic value of cardiac hybrid imaging integrating single-photon emission computed tomography with coronary computed tomography angiography. Eur Heart J 2011;32:1465–71.
27. Christou MA, Siontis GC, Katritsis DG, Ioannidis JP. Meta-analysis of fractional flow reserve versus quantitative coronary angiography and noninvasive imaging for evaluation of myocardial ischemia. Am J Cardiol 2007; 99:450–6.
28. Tonino PA, Fearon WF, De Bruyne B, et al. Angiographic versus functional severity of coronary artery stenoses in the FAME study fractional flow reserve versus angiography in multivessel evaluation. J Am Coll Cardiol 2010;55:2816–21.
29. Melikian N, De Bondt P, Tonino P, et al. Fractional flow reserve and myocardial perfusion imaging in patients with angiographic multivessel coronary artery disease. J Am Coll Cardiol Intv 2010;3:307–14.

30. Jung PH, Rieber J, Stork S, et al. Effect of contrast application on interpretability and diagnostic value of dobutamine stress echocardiography in patients with intermediate coronary lesions: comparison with myocardial fractional flow reserve. Eur Heart J 2008;29:2536–43.

31. Koo BK, Erglis A, Doh JH, et al. Diagnosis of ischemia-causing coronary stenoses by noninvasive fractional flow reserve computed from coronary computed tomographic angiograms. Results from the prospective multicenter DISCOVER-FLOW (Diagnosis of Ischemia-Causing Stenoses Obtained Via Noninvasive Fractional Flow Reserve) study. J Am Coll Cardiol 2011;58:1989–97.

32. Min JK, Leipsic J, Pencina MJ, et al. Diagnostic accuracy of fractional flow reserve from anatomic CT angiography. JAMA 2012;308:1237–45.

33. Watkins S, McGeoch R, Lyne J, et al. Validation of magnetic resonance myocardial perfusion imaging with fractional flow reserve for the detection of significant coronary heart disease. Circulation 2009;120:2207–13.

34. Zoghbi GJ, Dorfman TA, Iskandrian AE. The effects of medications on myocardial perfusion. J Am Coll Cardiol 2008;52:401–16.

Key Words: computed tomography ■ coronary disease ■ fractional flow reserve ■ imaging ■ ischemia ■ quantitative coronary angiography.